

## **Communications**







How to cite: Angew. Chem. Int. Ed. 2020, 59, 10379-10384 International Edition: doi.org/10.1002/anie.202001706 German Edition: doi.org/10.1002/ange.202001706

# Enhanced Single-Chain Magnet Behavior via Anisotropic Exchange in a Cyano-Bridged Mo<sup>III</sup>-Mn<sup>II</sup> Chain

Le Shi, Dong Shao, Xiao-Qin Wei, Kim R. Dunbar,\* and Xin-Yi Wang\*

Dedicated to the 100th anniversary of the School of Chemistry and Chemical Engineering, Nanjing University

Abstract: Anisotropic magnetic exchange is of great value for the design of high performance molecular nanomagnets. In the present work, enhanced single-chain magnet (SCM) behavior is observed for a Mo<sup>III</sup>–Mn<sup>II</sup> chain that exhibits anisotropic magnetic exchange. Self-assembly of the pentagonal bipyramidal  $[Mo(CN)_7]^{4-}$  anion and the  $Mn^{II}$  unit with a tridentate ligand results in a neutral double zigzag 2,4-ribbon structure which exhibits SCM behavior with a high relaxation barrier of 178(4) K. Open magnetic hysteresis loops are observed below 5.2 K, with a coercive field of 1.5 T at 2 K. Interestingly, this SCM can be considered to be a result of a step-wise process based on our previously reported Mn<sub>2</sub>Mo single-molecule magnets (SMMs).

Since the experimental realization of Glauber dynamics in one-dimensional (1D) magnetic polymers, [1] single-chain magnets (SCMs) have attracted considerable attention as alternatives to single-molecule magnets (SMMs) for potential applications in spintronics and storage devices.<sup>[2]</sup> For both SMMs and SCMs, the relaxation energy barrier  $(\Delta_{\tau})$  is of crucial importance for their practical applications. For SMMs whose magnetic relaxation is governed by the Orbach mechanism, the  $\Delta_{\tau}$  is determined by the magnetic anisotropy of the metal ions or multinuclear metal compounds, while other mechanisms such as Raman, direct and quantum tunneling of the magnetization (QTM) can also play important roles. [3] In contrast, the  $\Delta_{\tau}$  of an SCM has contributions from both the local energy barrier  $\Delta_A$  from the intrinsic magnetic anisotropy of the spin units and the correlation energy  $\Delta_{\varepsilon}$  from the intrachain magnetic coupling  $J^{[4]}$  Therefore, it should be easier, in principle, to increase  $\Delta_{\tau}$  of the SCMs by enhancing both the local magnetic anisotropy and the intrachain magnetic coupling.<sup>[5]</sup> This strategy has led to a number of high performance SCMs prepared by connecting highly anisotropic magnetic units, such as those containing Co<sup>II</sup>, Mn<sup>III</sup> and Ln<sup>III</sup> ions or polynuclear molecules behaving as SMM themselves (for example, Mn<sub>2</sub>Fe, [6] Mn<sub>3</sub>, [7] and Mn<sub>4</sub> SMMs<sup>[8]</sup>), with bridges such as nitronyl nitroxides<sup>[9]</sup> and organonitrile<sup>[10]</sup> radicals, azides, <sup>[11]</sup> and cyanides as well as others.[12-15]

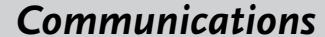
Among the reported SCMs, the 4d and 5d cyanometallate complexes are of special interest. [16] Benefitting from their large spin-orbit coupling and more diffuse d orbitals compared to the 3d ions, these heavier metal spin centers can provide both high magnetic anisotropy and strong magnetic exchange. Indeed, high barrier 4d and 5d SCMs have been realized, with examples being prepared from [Ru(acac)<sub>2</sub>- $(CN)_2$ ]<sup>-,[17]</sup>  $[Os(CN)_6]^{3-,[18]}$   $[ReCl_4(CN)_2]^{2-,[19]}$  and [M-] $(CN)_8$ ]<sup>3-/4-</sup> (M = Mo, W, Nb) units.<sup>[20-23]</sup> The new record of  $\Delta_{\tau}$  for cyanide-bridged SCMs ( $\Delta_{\tau} = 252 \text{ K}$ ) was reported for a Co<sup>II</sup>–W<sup>V</sup> compound by some of us in 2016.<sup>[21]</sup>

In this vein, the  $[Mo^{III}(CN)_7]^{4-}$  unit is a very attractive starting material as evidenced by the fact that strong exchange between MoIII spins with other metal ions through bridging cyanide groups leads to high  $T_c$  magnets<sup>[24]</sup> with the highest  $T_c$  value being 110 K for a V<sup>II</sup>-Mo<sup>III</sup> compound. [24f] In the context of the present study, the strong anisotropic Mo<sup>III</sup>– CN-Mn<sup>II</sup> exchange interaction, which was first theoretically proposed, [25] was experimentally confirmed to be promising for the preparation of high  $T_{\rm B}$  SMMs by Dunbar and Wang. [26] In these studies a docasanuclear  $Mn_{14}Mo_8$  cluster with an S =31 ground state was obtained, [27] as well as a [Mo(CN)<sub>7</sub>]<sup>4-</sup> based Mn<sub>2</sub>Mo trinuclear SMM with a record barrier for a cyano-bridged SMM in 2013. [26] In the case of the latter SMM, both Mn<sup>II</sup> ions are connected to the apical CN<sup>-</sup> groups of the pentagonal bipyramid (PBPY) [Mo(CN)<sub>7</sub>]<sup>4-</sup> unit which leads to strong anisotropic magnetic exchange, an important observation for future design considerations. Theoretical analyses revealed that the Mo<sup>III</sup>-CN-Mn<sup>II</sup> magnetic interactions can be described by the anisotropic Hamiltonian  $\hat{H}_{ ext{eff}}$  =  $-J_{xy}(S^x_{Mo}S^x_{Mn} + S^y_{Mo}S^y_{Mn}) - J_zS^z_{Mo}S^z_{Mn}$ . An Ising-type interaction  $(J_z/hc = -17 \text{ cm}^{-1}, J_{xy}/hc = -5.5 \text{ cm}^{-1}, \text{ and } |J_z| > |J_{xy}|)$  is operative for the apical Mo-CN-Mn pairs and is responsible for its uniaxial magnetic anisotropy and SMM behavior. Importantly, the anisotropic exchange can be efficiently tuned by modifying either the local geometry of Mo<sup>III</sup> or the bridging modes of [Mo<sup>III</sup>(CN)<sub>7</sub>]<sup>4-</sup> to the Mn<sup>II</sup> ions. In fact, two related equatorially connected Mn<sub>2</sub>Mo compounds exhibit only simple paramagnetic behavior. Even more remarkable is the fact that for Mn<sub>2</sub>Mo and Mn<sub>4</sub>Mo<sub>2</sub> compounds ([Mn(L)- $(H_2O)]_2[Mo(CN)_7]\cdot 2H_2O$  and  $[Mn(L)(H_2O)]_2[Mn(L)]_2[Mo-$ (CN)<sub>7</sub>]<sub>2</sub>), the SMM behavior can be switched on and off by

Department of Chemistry, Texas A & M University College Station, TX 77840 (USA) E-mail: dunbar@chem.tamu.edu

Supporting information and the ORCID identification number(s) for the author(s) of this article can be found under https://doi.org/10. 1002/anie.202001706.

<sup>[\*]</sup> L. Shi, Dr. D. Shao, Dr. X. Q. Wei, Prof. Dr. X. Y. Wang State Key Laboratory of Coordination Chemistry, Collaborative Innovation Center of Advanced Microstructures, School of Chemistry and Chemical Engineering, Nanjing University Nanjing, 210023 (China) E-mail: wangxy66@nju.edu.cn Prof. Dr. K. R. Dunbar

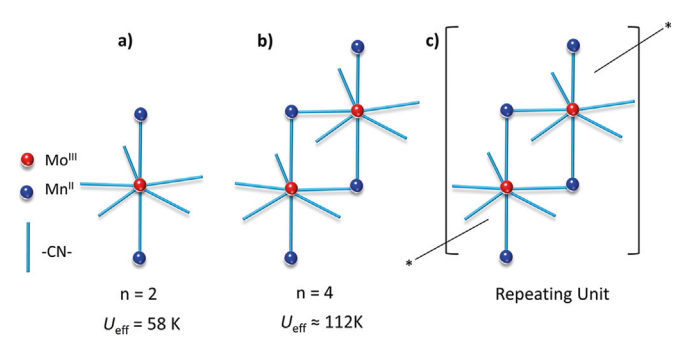






changing the local geometry of the Mo<sup>III</sup> center, which disrupts the anisotropic exchange interaction.<sup>[28]</sup>

Inspired by these achievements, we turned our attention to the preparation of high barrier SCMs based on  $[Mo^{III}-(CN)_7]^{4-}$  by taking advantage of strong anisotropic exchange coupling. In terms of the promise for this idea, we noted with interest that, after the report of our  $Mn_2Mo$  SMM (Scheme 1a), Mironov performed calculations that led to the



**Scheme 1.** a) Schematic view of the trinuclear  $Mn_2Mo$  SMM; b) Calculated  $Mn_4Mo_2$  skeleton composed of two linear  $Mn_2Mo$  units coupled via the equatorial cyanides; c) Possible 1D assembly composed of  $Mn_2Mo$  units.

prediction that much higher  $\Delta_{\tau}$  values would be obtained by connecting the Mn<sub>2</sub>Mo SMMs to form higher nuclearity molecules (Scheme 1b).<sup>[29]</sup> With this intriguing possibility in mind, we hypothesized that a one-dimensional assembly composed of Mn<sub>2</sub>Mo magnetic units (Scheme 1c) could behave as an SCM with a high relaxation barrier. Herein, we report the preparation of the SCM, [Mn(bida)(H<sub>2</sub>O)]<sub>2</sub>- $[Mo(CN)_7] \cdot 6H_2O$  (1, bida = 1,4-bis(4-imidazolyl)-2,3-diaza-1,3-butadiene). The bida ligand was chosen because of our recent successful preparation of the Mn<sub>2</sub>Mo and Mn<sub>4</sub>Mo<sub>2</sub> compounds with similar bis(imidazolylimine) ligands.<sup>[28]</sup> Magnetic investigations reveal a high barrier of 178(4) K and open hysteresis loops up to 5.2 K, which are the second highest values among all cyano-bridged SCMs. Unlike other reported SCMs, strong anisotropic Mo<sup>III</sup>-Mn<sup>II</sup> exchange coupling contributes to both  $\Delta_A$  and  $\Delta_{\xi}$ .

Orange platelet crystals of 1 were prepared by slow diffusion of an acetonitrile solution of  $Mn(ClO_4)_2 \cdot 6H_2O$  and bida into an aqueous solution of  $K_4Mo(CN)_7 \cdot 2H_2O$  in a test tube under a nitrogen atmosphere (see details in the Supporting Information). The phase purity of the complex was confirmed by powder X-ray diffraction (Figure S1 in the Supporting Information). The slow diffusion method is essential for obtaining samples with high crystallinity and purity. Although the stoichiometry of the reactants was not strict for the crystal growth, we chose the stoichiometric 2:2:1 molar ratio of  $Mn^{2+}$ :bida: $[Mo(CN)_7]^{4-}$  because it provided the best yields.

Compound **1** crystallizes in the triclinic space group  $P\overline{1}$  (Table S1). The asymmetric unit contains one  $[Mo(CN)_7]^{4-}$  anion with PBPY geometry, two  $[Mn(bida)(H_2O)]^{2+}$  moieties bound to two apical  $CN^-$  groups, and six interstitial water molecules (Figure 1 and S4). The asymmetric  $Mn_2Mo$  unit is very similar to the two reported  $Mn_2Mo$  SMMs. [26,28] Impor-

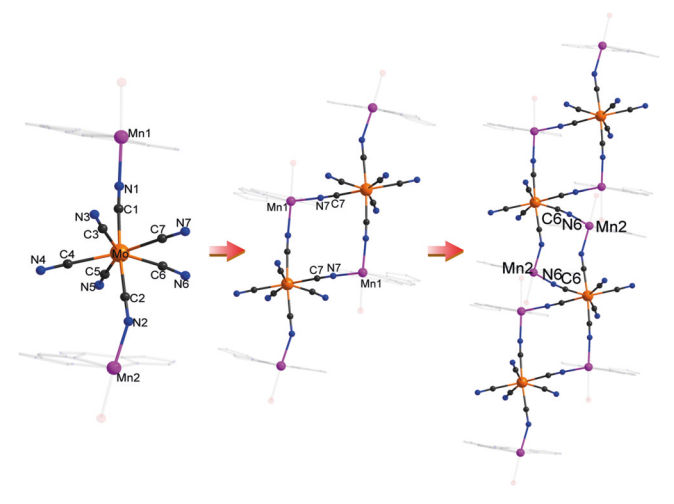


Figure 1. Step-wise view of the structure of 1: from trinuclear to hexanuclear to the 1D chain. All hydrogen atoms and solvent molecules were omitted for the sake of clarity.

tant geometrical parameters of  $[Mo(CN)_7]^{4-}$  anion are the axial C-Mo-C bond angles (175.2(4)°), and the adjacent C-Mo-C angles in the equatorial planes (70.9(4)° –74.6(4)°, Table S2) both of which indicate a slightly distorted PBPY geometry as confirmed by the calculated continuous shape measure (CShMs) value (0.638, Table S3) of the Mo<sup>III</sup> center. This axial PBPY geometry is very important from the magnetic perspective since the ideal geometry exhibits the greatest potential for anisotropic magnetic exchange. [25] The two Mn<sup>II</sup> centers, Mn1 and Mn2, reside in distorted octahedra (CShMs = 1.806 and 1.649, respectively, Table S3).

Each [Mo(CN)<sub>7</sub>]<sup>4-</sup> anion is connected to four Mn<sup>II</sup> centers through two apical (C1N1 and C2N2) and two equatorial (C6N6 and C7N7) CN groups and each Mn<sup>II</sup> unit is connected to two Mo<sup>III</sup> centers. For the Mo-C-N-Mn linkages, the Mo-C-N angles are close to 180°, whereas the C-N-Mn angles ( $\theta$ ) are significantly bent (156.0(1)-177.7(5)°), which, according to the theoretical studies, [29] is closely related to the Mo<sup>III</sup>-Mn<sup>II</sup> exchange interaction. These connectivities lead to a neutral double zigzag 2,4-ribbon chain with vertex-sharing Mn<sub>2</sub>Mo<sub>2</sub> squares as repeating units. Actually, the chain can best be described as a 1D assembly of the repeating apical Mn1-Mo1-Mn2 units connected by the equatorial CN groups (Figure 1). Because of the similarity of the Mn<sub>2</sub>Mo unit in 1 with the two reported Mn<sub>2</sub>Mo SMMs<sup>[26,28]</sup> (see details in Figure S5), "SMM" behavior of the Mn<sub>2</sub>Mo unit in 1 is reasonably anticipated. Therefore, the chain of 1 can be viewed as a 1D array of the Mn<sub>2</sub>Mo SMMs. Although weak interchain interactions, namely hydrogen bonds involving the water molecules and the terminal CN groups (Figure S6) are present, there are no close metal-metal contacts; the shortest interchain metal-metal distances are 8.698(4), 10.274(5), and 7.601(8) Å for Mo<sup>III</sup>-Mn<sup>II</sup>, Mo<sup>III</sup>-Mo<sup>III</sup> and Mn<sup>II</sup>-Mn<sup>II</sup> ions, respectively.

Variable-temperature magnetic susceptibility measurements on powders prepared by grinding single crystal samples were performed on **1**. A plot of  $\chi_{\rm M} T$  vs. T, collected under a direct current (dc) field of 1000 Oe, is depicted in Figure 2.



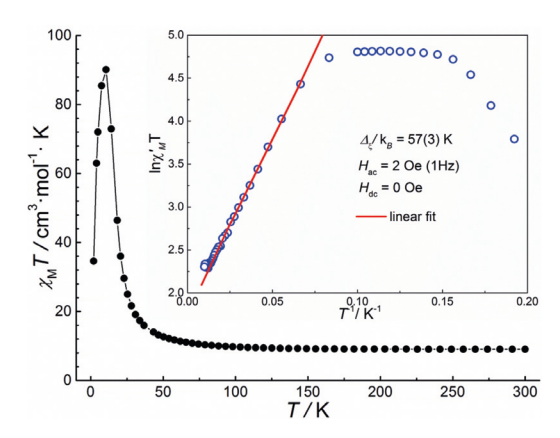


Figure 2. Variable-temperature dc magnetic susceptibility data for 1 measured under 1 kOe. Inset: Plot of  $\ln(\chi'_{\rm M}T)$  vs. 1/T. The red line corresponds to a linear fit of the data.

At 300 K, the  $\chi_M T$  value (9.05(1) cm<sup>3</sup> K mol<sup>-1</sup>) is slightly lower than the expected spin-only value (9.125 cm<sup>3</sup> K mol<sup>-1</sup>) for one low-spin Mo<sup>III</sup> center (S = 1/2) and two high-spin Mn<sup>II</sup> centers (S = 5/2). Upon cooling,  $\chi_{\rm M} T$  increases gradually until  $\approx 50$  K, and then more abruptly to a maximum of 90.1(1) cm<sup>3</sup> K mol<sup>-1</sup> at 10 K, followed by a decrease to 34.59(2) cm<sup>3</sup> K mol<sup>-1</sup> at 2 K. The decrease is attributed to magnetization freezing at low temperature (vide post). Although this  $\chi_M T$  curve suggests a dominant effective Mo<sup>III</sup>-Mn<sup>II</sup> ferromagnetic coupling, antiferromagnetic Mo<sup>III</sup>-Mn<sup>II</sup> interactions have been experimentally and theoretically confirmed in several MnII-[MoIII-(CN)<sub>7</sub>]<sup>4-</sup> compounds. [26-28,30] Hence, we believe that the Mo<sup>III</sup>– Mn<sup>II</sup> interaction in 1 is also antiferromagnetic, leading to the ferrimagnetic arrangement of the spins. This conclusion is supported by the M(H) curve measured at 2.0 K (Figure S7) as the magnetization is not saturated at even 70 kOe, reaching a highest value of 7.54  $\mu_{\!\scriptscriptstyle B}\!.$  This value is slightly lower than the expected 9.0  $\mu_B$  for a ferrimagnetic state, but is much lower than  $11 \mu_B$  for a ferromagnetic alignment. In addition, the magnetic interaction between the Mn<sup>II</sup> and the PBPY Mo<sup>III</sup> spins should be highly anisotropic. For all four different magnetic pathways (C1N1 and C7N7 for Mo1-Mn1, and C2N2 and C6N6 for Mo1-Mn2), eight  $J_z$  and  $J_{xy}$  parameters are thus needed which precludes a quantitative modelling of the data. According to the previously reported theoretical work however, [25,29] for the apical Mo<sup>III</sup>-CN-Mn<sup>II</sup> pairs the magnetic interaction should be Ising-type with  $|J_z| > |J_{xy}|$ .

To probe the magnetic dynamics of 1, temperature- and frequency-dependent ac susceptibilities were measured. As shown in Figure 3a and Figure S8, S9, strong frequency dependent in-phase  $(\chi_M)$  and out-of-phase  $(\chi_M)$  signals were observed. The shift of the peak temperature  $(T_p)$  of  $\chi_M$ ", evaluated by the Mydosh parameter  $\phi = (\Delta T_p / T_p) / \Delta (\log f)$  $\approx\!0.14,$  is in a normal range for an SCM.  $^{[31]}$  The ac data from 5.6 to 10.0 K were used to construct Cole-Cole plots (Figure S10) which were analyzed by the generallized Debye model. [32] The  $\alpha$  parameters (0.18–0.52, Table S4) indicate a relative broad distribution of relaxation times  $\tau$ , which is attributed to a distribution of the chain length in 1. Since the magnetic relaxation is slow below 5.6 K, the dc magnetization decay was measured over the temperature range of 3.0 to

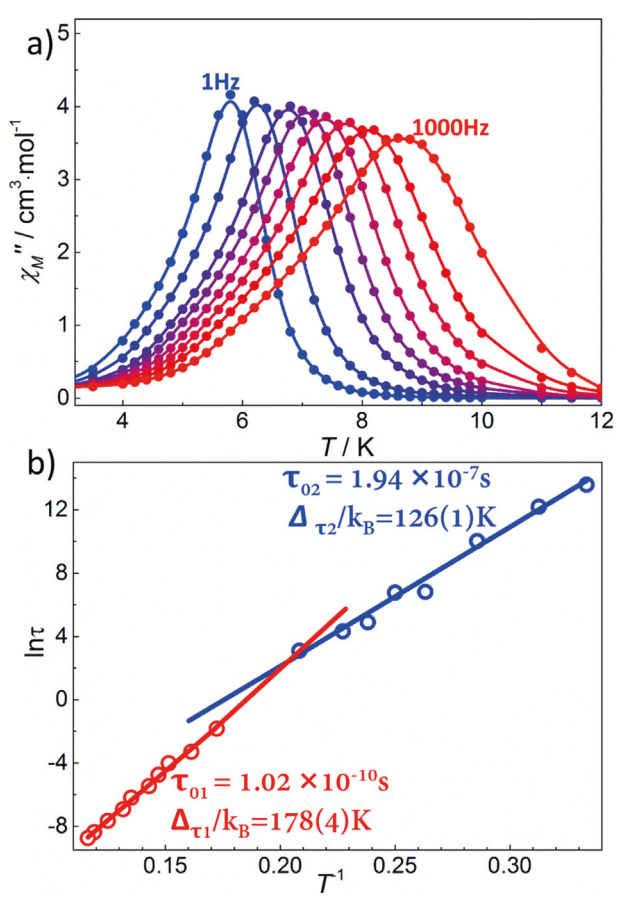
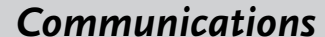


Figure 3. a) Variable-temperature out-of-phase ac magnetic susceptibility data ( $\chi_{\rm M}''$ ) for 1 under  $H_{\rm dc} = 0$  Oe,  $H_{\rm ac} = 2$  Oe; b) Relaxation time of 1 derived from the ac data (red) and time dependent dc magnetization (blue). The solid lines correspond to the linear fit according to the Arrhenius law.

4.8 K. As shown in Figure S11, the data are best described by a streched exponential decay  $(M(t) = M_0 - \exp[(t/\tau)^B])$  to give the  $\tau$  values.<sup>[33]</sup> An Arrehenius plot of  $\ln \tau$  vs.  $T^{-1}$  (Figure 3b) was obtained from both the ac and dc results and there are two distinct thermally activated regions, corresponding to the infinite-size and finite-size regimes of relaxation as commonly observed for SCMs, [4,5] with the crossover temperature of  $T^* = 4.9$  K. The  $\Delta_{\tau}$  for both regimes were estimated using the Arrhenius law  $\tau = \tau_0 \exp(\Delta_{\tau}/k_B T)$ , giving  $\Delta_{\tau 1} = 178(4)$  K and  $\tau_{01} = 1.02 \times 10^{-10}$  s, and  $\Delta_{\tau 2} = 126(1)$  K and  $\tau_{02} = 1.94 \times 10^{-7}$  s.

For a chain compound with strong anisotropy, such as the commonly studied anisotropic Heisenberg or Ising model chains,  $\chi_{\rm M} T$  is directly proportional to the correlation length  $\xi$ , and follows the equation  $\chi_{\rm M} T = C_{\rm eff} \exp(\Delta_{\xi}/k_{\rm B} T)$ , where  $\Delta_{\xi}$ is the energy required to create a domain wall and  $C_{
m eff}$  is the effective Curie constant per magnetic unit.<sup>[4,5]</sup> Therefore, the ac susceptibility data from 2 to 60 K were measured under a  $H_{\rm ac} = 2$  Oe and  $H_{\rm dc} = 0$  Oe field at a frequency of 1 Hz. As expected, the  $ln(\chi'_M T)$  vs. 1/T plot (inset of Figure 2) exhibits a linear region from 16 to 60 K, yielding  $\Delta_{\xi}/k_{\rm B} = 57(3)$  K and  $C_{\rm eff} = 6.04 \, {\rm cm}^3 \, {\rm K \, mol}^{-1}$ . Below 15 K, the  $\ln(\chi'_{\rm M} T)$  is saturated and remains nearly constant down to 6.8 K, after which temperature it decreases to 2 K. We note that the crossover

10381







temperature  $T^*$  estimated here (  $\approx 10 \text{ K}$ ) is apparently higher than the  $T^*$  obtained above (4.9 K) from the dynamic data. This has been reported for other SCMs and can originate from weak antiferromagnetic interactions between the chains or chain segments. [18,34] The saturation of the  $\chi'_{M}T$  value reflects the finite-size effect due to the naturally occurring defects in the chain; the further decrease can be attributed to weak AF interchain interactions. From the maximum value of  $\chi'_{M} T$  and  $C_{\text{eff}}$ , the number of the repeating unit n of the Mn<sub>2</sub>Mo units in a chain segment can be estimated by  $n = (\chi'_{\rm M} T)_{\rm max}/C_{\rm eff} \approx 20$ , which corresponds to an average chain length of  $L \approx 14$  nm. According to the theoretical prediction, the overall energy barrier  $\Delta_{\tau}$  for an SCM is  $\Delta_{\tau 1} = 2\Delta_{\xi} + \Delta_{A}$  for the infinite chain at high temperature and  $\Delta_{\tau 2} = \Delta_{\xi} + \Delta_{A}$  for the finite-size chain at low temperature. [35,36] From the obtained  $\Delta_{\tau 1}$  and  $\Delta_{\tau 2}$  values,  $\Delta_{\varepsilon}$  can be calculated by  $\Delta_{\varepsilon} = \Delta_{\tau 1} - \Delta_{\tau 2} = 52$  K, which is in good agreement with the value of 57 K obtained above. In addition, the intrinsic anisotropic barrier  $\Delta_A$  can be calculated by  $\Delta_A$  =  $\Delta_{\tau 1} - 2\Delta_{\xi} = 64 \text{ K or } \Delta_{A} = \Delta_{\tau 2} - \Delta_{\xi} = 66 \text{ K}$ . These values are close to those reported for the two trinuclear Mn<sub>2</sub>Mo SMMs (58.5 K and 64.6 K).[26,28]

To confirm the SCM behaviour of 1, zero-field-cooled (ZFC) and field-cooled (FC) magnetic susceptibility data under a dc field of 10 Oe and magnetic hysteresis loops below 5.2 K were measured. As depicted in Figure S12, the ZFC and FC curves sharply diverge at 5.8 K. Hysteresis data were measured using both powders from ground single crystals and a collection of single crystals (8.1 mg) oriented in a strong magnetic field. The single crystals embedded in eicosane were oriented in a magnetic field of 7 T at 315 K (42°C) for 5 minutes before being cooled with the field on. Magnetic measurements were then performed at 2.0 to 5.2 K at different field sweep rates (Figure 4 and Figure S13). Temperature- and field-sweep-rate dependent magnetic hysteresis loops were observed, with the coercive field  $H_{\rm c}$  increasing with lowering temperature and increasing field sweep rate. At a field sweep rate of 100 Oe s<sup>-1</sup> (Figure 4), the loop of the oriented single crystals remains open until  $\approx 5.2$  K and the  $H_c$ 

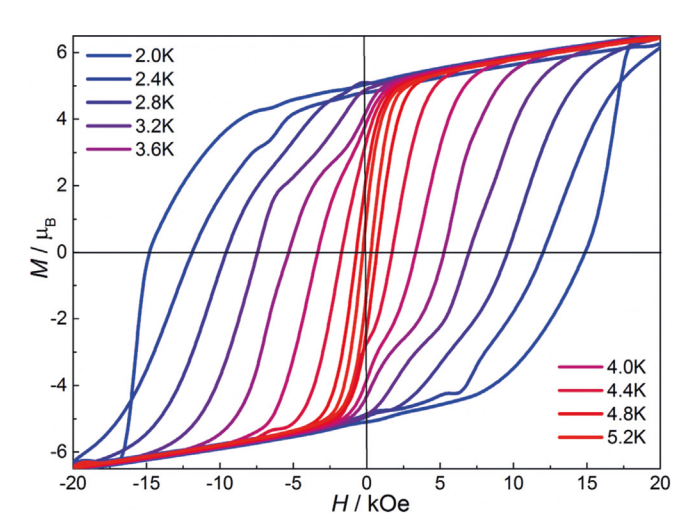


Figure 4. Magnetic hysteresis loops measured at a sweep rate of 100 Oe s<sup>-1</sup> at 2.0 to 5.2 K on a collection of field oriented single crystals of 1.

reaches 1.5 T at 2 K. Interestingly the loops at 2.8 to 4.4 K exhibit obvious steps, which shift to higher magnetic field as the temperature is lowered. Such steps in the loops indicate rapid relaxation at specific fields, which has been observed frequently in SMMs corresponding to resonant quantum tunnelling of the magnetization.

All these aforementioned data unambiguously confirm that 1 behaves as an SCM. Apart from the remarkably high energy barrier and blocking temperature, several aspects of 1 warrant further comments. As described for the two reported Mn<sub>2</sub>Mo SMMs, the magnetic anisotropy necessarily arises from anisotropic magnetic exchange since the low spin  $Mo^{III}$  (S = 1/2) does not have zero-field splitting and the D value of the Mn<sup>II</sup> centers is expected to be very small. In this case, the effective Hamiltonian for 1 cannot be described by either the Ising model or the anisotropic Heisenberg model unlike most of the reported SCMs. Clearly theoretical studies for SCMs based on anisotropic exchange are required to fully understand the detailed mechanisms. This situation notwithstanding, the magnetic anisotropy in 1 can be described as the easy-axis type since the SCM is assembled from Mn<sub>2</sub>Mo units that resemble the reported SMMs.

A second important point is that, although the domain wall (DW) structure for an SCM is typically based on the relative magnitude of the D and J parameters, this approach is not applicable in the present case. A threshold between narrow and broad DW regions occurs for |D/J| = 4/3 ( $|D/J| \ge$ 4/3 for the Ising limit and  $|D/J| \ll 4/3$  for the Heisenberg limit). [4b,5,36] The easy-axis magnetic anisotropy in **1**, however, is directly related to the magnetic coupling, which precludes the assignment of the DW structure of 1.

A third issue to address is the high performance of the SCM behaviour of 1 compared to reported SCMs. The properties of 1 are remarkable vis-à-vis the high barrier and blocking temperature as compared to a previously reported cyano-bridged Mo<sup>III</sup>-Mn<sup>II</sup> SCM which exhibits a much lower energy barrier of 69.5 K.[37] This difference is directly related to the bridging modes of  $[Mo^{III}(CN)_7]^{4-}$  to the  $Mn^{II}$  ions. The relatively large correlation energy  $\Delta_{\epsilon}$  reflects the efficient Mo<sup>III</sup>-Mn<sup>II</sup> magnetic exchange through the CN<sup>-</sup> bridges. For the local anisotropic barrier  $\Delta_A$ , this value is correlated with the energy barriers of the Mn<sub>2</sub>Mo SMMs. Furthermore, the observed steps in the hysteresis loops in 1 are reminiscent of the QTM steps observed in the Mn<sub>2</sub>Mo SMM.<sup>[26]</sup> All of these observations, taken together, verify that the SMM behaviour from anisotropic exchange is preserved in the SCM which nicely confirms the strategy of connecting the SMMs to form

In summary, a novel  $[Mo(CN)_7]^{4-}$  based SCM has been synthesized and its SCM behavior confirmed by both static and dynamic magnetic measurements. This SCM can be viewed as a 1D array of the first reported Mn<sub>2</sub>Mo SMM published by these authors which hints at the potential for designing molecular nanomagnets based on the [Mo(CN)<sub>7</sub>]<sup>4-</sup> unit. Importantly, the magnetic anisotropy of this SCM originates from anisotropic magnetic exchange involving the axial cyanide ligands of the pentagonal bipyramidal Mo<sup>III</sup> unit and the Mn<sup>II</sup> spins. The effective energy barrier and the blocking temperature are significantly larger than most

## Communications





reported cyanide-based SCMs. This new SCM constitutes an interesting example of SCMs beyond the Glauber model. Further experimental and theoretical studies of this new compound are in progress. Efforts to prepare more high performance SCMs using the  $[Mo(CN)_7]^{4-}$  anion in chain architectures with other paramagnetic metal centers are also underway, particularly those which are expected to be strongly coupled to the Mo<sup>III</sup> center though the cyanide ligands.

#### Acknowledgements

X.-Y.W. acknowledges funding from the National Key R&D Program of China (2018YFA0306002) and NSFC (21973039 and 21522103). K.R.D. thanks the National Science Foundation (CHE-1808779) and Welch Foundation (A-1449) for support. D.S. thanks the Postgraduate Research & Practice Innovation Program of Jiangsu Province (KYCX19\_0033) and the China Postdoctoral Science Foundation (2018M640473).

### Conflict of interest

The authors declare no conflict of interest.

**Keywords:** cyanometallate · heptacyanomolybdate · molecule magnetism · pentagonal bipyramid · single-chain magnet

- [1] A. Caneschi, D. Gatteschi, N. Lalioti, C. Sangregorio, R. Sessoli, G. Venturi, A. Vindigni, A. Rettori, M. G. Pini, M. A. Novak, Angew. Chem. Int. Ed. 2001, 40, 1760-1763; Angew. Chem. **2001**, 113, 1810 – 1813.
- [2] D. Gatteschi, R. Sessoli, J. Villain, Molecular Nanomagnets, Oxford University Press, Oxford, UK, 2006.
- [3] D. Gatteschi, R. Sessoli, Angew. Chem. Int. Ed. 2003, 42, 268-297; Angew. Chem. 2003, 115, 278-309.
- [4] a) R. Clérac, H. Miyasaka, M. Yamashita, C. Coulon, J. Am. Chem. Soc. 2002, 124, 12837 - 12844; b) C. Coulon, H. Miyasaka, R. Clérac, Struct. Bonding (Berlin) 2006, 122, 163.
- [5] a) H.-L. Sun, Z.-M. Wang, S. Gao, Coord. Chem. Rev. 2010, 254, 1081; b) W.-X. Zhang, R. Ishikawa, B. Breedlove, M. Yamashita, RSC Adv. 2013, 3, 3772 – 3798; c) M. Böhme, W. Plass, Chem. Sci. **2019**. 10. 9189 - 9202.
- [6] M. Ferbinteanu, H. Miyasaka, W. Wernsdorfer, K. Nakata, K. Sugiura, M. Yamashita, C. Coulon, R. Clérac, J. Am. Chem. Soc. **2005**, 127, 3090 – 3099.
- [7] H.-B. Xu, B.-W. Wang, F. Pan, Z.-M. Wang, S. Gao, Angew. Chem. Int. Ed. 2007, 46, 7388-7392; Angew. Chem. 2007, 119, 7532 - 7536.
- [8] L. Lecren, O. Roubeau, C. Coulon, Y.-G. Li, X. Le Goff, W. Wernsdorfer, H. Miyasaka, R. Clérac, J. Am. Chem. Soc. 2005, 127, 17353-17363.
- [9] a) F. Houard, Q. Evrard, G. Calvez, Y. Suffren, C. Daiguebonne, O. Guillou, F. Gendron, B. Guennic, T. Guizouarn, V. Dorcet, M. Mannini, K. Bernot, Angew. Chem. Int. Ed. 2020, 59, 780-784; Angew. Chem. 2020, 132, 790-794; b) X. Meng, W. Shi, P. Cheng, Coord. Chem. Rev. 2019, 378, 134-150.

- [10] Z.-X. Wang, X. Zhang, Y.-Z. Zhang, M.-X. Li, H. Zhao, M. Andruh, K. R. Dunbar, Angew. Chem. Int. Ed. 2014, 53, 11567 -11570; Angew. Chem. 2014, 126, 11751-11754.
- [11] a) H.-B. Xu, B.-W. Wang, F. Pan, Z.-M. Wang, S. Gao, Angew. Chem. Int. Ed. 2007, 46, 7388-7392; Angew. Chem. 2007, 119, 7532-7536; b) X.-H. Zhao, L.-D. Deng, Y. Zhou, D. Shao, D.-Q. Wu, X.-Q. Wei, X.-Y. Wang, Inorg. Chem. 2017, 56, 8058-8067.
- [12] a) C. Pichon, N. Suaud, C. Duhayon, N. Guihéry, J. P. Sutter, J. Am. Chem. Soc. 2018, 140, 7698-7704; b) D. Shao, S.-L. Zhang, X.-H. Zhao, X.-Y. Wang, Chem. Commun. 2015, 51, 4360 – 4363.
- [13] a) Y.-Z. Zhang, H.-H. Zhao, E. Funck, K. R. Dunbar, Angew. Chem. Int. Ed. 2015, 54, 5583-5587; Angew. Chem. 2015, 127, 5675-5679; b) D.-P. Dong, T. Liu, S. Kanegawa, S. Kang, O. Sato, C. He, C.-Y. Duan, Angew. Chem. Int. Ed. 2012, 51, 5119-5123; Angew. Chem. 2012, 124, 5209-5213.
- [14] J. A. DeGayner, K. Wang, T. D. Harris, J. Am. Chem. Soc. 2018, 140, 6550 - 6553.
- [15] V. Mougel, L. Chatelain, J. Hermle, R. Caciuffo, E. Colineau, F. Tuna, N. Magnani, A. de Geyer, J. Pécaut, M. Mazzanti, Angew. Chem. Int. Ed. 2014, 53, 819 – 823; Angew. Chem. 2014, 126, 838 – 842.
- [16] X.-Y. Wang, C. Avendańo, K. R. Dunbar, Chem. Soc. Rev. 2011, 40, 3213-3238
- [17] J.-F. Guo, X.-T. Wang, B.-W. Wang, G.-C. Xu, S. Gao, L. Szeto, W.-T. Wong, W.-Y. Wong, T.-C. Lau, Chem. Eur. J. 2010, 16, 3524 - 3535
- [18] E. V. Peresypkina, A. M. Majcher, M. Rams, K. E. Vostrikova, Chem. Commun. 2014, 50, 7150-7153.
- [19] a) T. D. Harris, M. V. Bennett, R. Clérac, J. R. Long, J. Am. Chem. Soc. 2010, 132, 3980-3988; b) X. Feng, T. D. Harris, J. R. Long, Chem. Sci. 2011, 2, 1688-1694; c) X. Feng, J. Liu, T. D. Harris, S. Hill, J. R. Long, J. Am. Chem. Soc. 2012, 134, 7521 -7529.
- [20] Y.-Z. Zhang, B. S. Dolinar, S. Liu, A. J. Brown, X. Zhang, Z.-X. Wang, K. R. Dunbar, Chem. Sci. 2018, 9, 119-124.
- [21] R.-M. Wei, F. Cao, J. Li, L. Yang, Y. Han, X.-L. Zhang, Z. Zhang, X.-Y. Wang, Y. Song, Sci. Rep. 2016, 6, 24372.
- [22] S. Chorazy, K. Nakabayashi, K. Imoto, J. Mlynarski, B. Sieklucka, S. Ohkoshi, J. Am. Chem. Soc. 2012, 134, 16151-16154.
- [23] T. S. Venkatakrishnan, S. Sahoo, N. Bréfuel, C. Duhayon, C. Paulsen, A. L. Barra, S. Ramasesha, J. P. Sutter, J. Am. Chem. Soc. 2010, 132, 6047-6056.
- [24] a) J. Larionova, R. Clérac, J. Sanchiz, O. Kahn, S. Gohlen, L. Ouahab, J. Am. Chem. Soc. 1998, 120, 13088-13095; b) O. Kahn, J. Larionova, L. Ouahab, Chem. Commun. 1999, 945-952; c) J. Larionova, O. Kahn, S. Gohlen, L. Ouahab, R. Clérac, J. Am. Chem. Soc. 1999, 121, 3349-3356; d) J. Larionova, R. Clérac, B. Donnadieu, C. Guérin, Chem. Eur. J. 2002, 8, 2712-2716; e) J. Milon, M. Daniel, A. Kaiba, P. Guionneau, S. Brandès, J.-P. Sutter, J. Am. Chem. Soc. 2007, 129, 13872-13878; f) K. Tomono, Y. Tsunobuchi, K. Nakabayashi, S. Ohkoshi, Inorg. Chem. 2010, 49, 1298-1300; g) D.-Q. Wu, D. Kempe, Y. Zhou, L.-D. Deng, D. Shao, X.-Q. Wei, L. Shi, K. R. Dunbar, X. Y. Wang, Inorg. Chem. 2017, 56, 7182-7189; h) L. Shi, D. Shao, F.-Y. Shen, X.-Q. Wei, X.-Y. Wang, Chin. J. Chem. 2019, 37, 19-24; i) M. Magott, K. R. Dunbar, D. Pinkowicz, Dalton Trans. 2019, 48, 15493 - 15500.
- [25] V. S. Mironov, L. F. Chibotaru, A. Ceulemans, J. Am. Chem. Soc. **2003**, 125, 9750 – 9760.
- [26] K. Qian, X.-C. Huang, C. Zhou, X.-Z. You, X.-Y. Wang, K. R. Dunbar, J. Am. Chem. Soc. 2013, 135, 13302-13305.
- [27] X.-Y. Wang, A. V. Prosvirin, K. R. Dunbar, Angew. Chem. Int. Ed. 2010, 49, 5081-5084; Angew. Chem. 2010, 122, 5207-5210.
- [28] D.-Q. Wu, D. Shao, X.-Q. Wei, F.-X. Shen, L. Shi, D. Kempe, Y.-Z. Zhang, K. R. Dunbar, X.-Y. Wang, J. Am. Chem. Soc. 2017, *139*, 11714-11717.

10383



## **Communications**



- [29] V. S. Mironov, Inorg. Chem. 2015, 54, 11339-11355.
- [30] B. Gillon, A. Goujon, S. Willemin, J. Larionova, C. Desplanches, E. Ruiz, G. André, J. A. Stride, C. Guérin, Inorg. Chem. 2007, 46,
- [31] J. A. Mydosh, Spin Glasses: An Experimental Introduction, Taylor and Francis, London, 1993, p. 67.
- [32] K. S. Cole, R. H. Cole, J. Chem. Phys. 1941, 9, 341-351.
- [33] S. M. Aubin, N. R. Dilley, L. Pardi, J. Krzystek, M. W. Wemple, L. C. Brunel, M. B. Maple, G. Christou, D. N. Hendrickson, J. Am. Chem. Soc. 1998, 120, 4991-5004.
- [34] H. Miyasaka, T. Madanbashi, A. Saitoh, N. Motokawa, R. Ishikawa, M. Yamashita, S. Bahr, W. Wernsdorfer, R. Clérac, Chem. Eur. J. 2012, 18, 3942-3954.
- [35] L. Bogani, A. Caneschi, M. Fedi, D. Gatteschi, M. Massi, M. A. Novak, M. G. Pini, A. Rettori, R. Sessoli, A. Vindigni, Phys. Rev. Lett. 2004, 92, 207204.
- [36] L. Bogani, A. Vindigni, R. Sessoli, D. Gatteschi, J. Mater. Chem. **2008**, 18, 4750 – 4758.
- [37] K. Wang, B. Xia, Q.-L. Wang, Y. Ma, D.-Z. Liao, J. Tang, Dalton *Trans.* **2017**, *46*, 1042 – 1046.

Manuscript received: February 2, 2020 Revised manuscript received: March 22, 2020 Accepted manuscript online: March 23, 2020 Version of record online: April 15, 2020